http://ansinet.com/itj

ITJ

ISSN 1812-5638

INFORMATION TECHNOLOGY JOURNAL

ANSInet
Asian Network for Scientific Information
308 Lasani Town, Sargodha Road, Faisalabad - Pakistan

Information Technology Journal 12 (11): 2121-2129, 2013
ISSN 1812-5638 / DOI: 10.3923/itj.2013.2121.2129

A Modified Energy Detection Algorithm for S-band Electronic Surveillance

Zhilu Wu, Longshi Kong, Zhendong Yin and Shuying Li
School of Electronics and Information Technology, Harbin Institute of Technology,
Harbin, Heilongjiang 150001, China

Abstract: Spectrum sensing techniques have gained much attention due to their capabilities to improve the utilization of the spectrum and lay the foundation of cognitive radio. In this paper, a new kind of modified energy detection algorithm is proposed for the application on S-band uplink electronic surveillance. In this scheme, first, the uplink signal of Unified S-band Telemetry Tracking and Control is derived from Matlab simulation which is a multi-modulation signal of PCM-BPSK-PM. Then, a new kind of modified method is proposed based on the study of classical energy detection algorithm which makes use of ratio threshold and the coefficient of kurtosis. Simulation shows that the proposed method offers better performances than classical energy detection method to a certain extent. At last, some filters are used to confirm the central frequency of the uplink signal which is unified S-band telemetry tracking and control signal. The simulation results show that the proposed method is able to offer low estimation errors.

Key words: S-band uplink, energy detection, central frequency, kurtosis

INTRODUCTION

Cognitive Radio (CR) was proposed by Doctor Joseph Mitola III in his PhD. dissertation in 1999 (Mitola III *et al*., 2012). CR techniques have gained much attention due to their capability to reuse the spectrum and to solve the spectrum congestion nowadays. CR is often considered as the key to next generation communication system (Mao and Wolf, 2010; Liang *et al*., 2010). In classical spectrum management mechanism, most of the spectrum bands are exclusively allocated to a few particular customers which results in the exhaustion of limited frequency resource as wireless applications grow. However, in contrast to spectrum scarcity, many results show that spectrum utilization is often very low (Zhao and Swami, 2007). For example, in the U.S., only 2% of the spectrum is used at any given time and location (Chen *et al*., 2011). One feasible solution to solve the spectrum scarcity is opportunistic spectrum access which needs the help of spectrum sensing technique. Generally speaking, there are largely three categories of methods: energy detection, matched filter and cyclo-stationary feature detection (Ozdemir *et al*., 2008; Maleki and Leus, 2013; Appadwedula *et al*., 2008; Wang *et al*., 2011). Among them, the first one, energy detection, doesn't need any priory information, resulting in low complexity. It can be affected by noise uncertainties easily, so the detection probability can't meet our requirements in low SNR (the ratio of signal to noise).

Most of the previous work on energy detection focused on setting absolute threshold. However, in this paper, a new method is presented to make it work well under low SNR. As coefficient of kurtosis is adopted, the new method differed from previous work in threshold setting. First, this study analyses the classical energy detection algorithm and proposes a modified method, where "Ratio threshold" is adopted. Simulations are run by using a multi-modulation signal of PCM-BPSK-PM which is used in S-bank uplink. Secondly, this paper compares the two methods, classical algorithm and modified algorithm. The results prove the feasibility of the modified algorithm. At last, we use "adding windows" method to estimate the central frequency of the carrier signal. The overall structure diagram is showed as follows. Figure 1 shows that: after receiving the signal of S-band uplink, we should carry out spectrum sensing by using energy detection algorithm. If there is no one using S-bank, go on searching. If we find S-bank uplink is used by someone, we will use "adding windows" method to estimate the carrier frequency.

SYSTEM MODEL

The input signal: In fact, S-band uplink monitoring and control signal (2025-2110 MHZ) is modulated in PCM-PSK-PM or PCM-PSK-FM form. In this paper, we use the former form: PCM-PSK-PM.

Corresponding Author: Zhendong Yin, School of Electronics and Information Technology, Harbin Institute of Technology, Harbin, Heilongjiang 150001, China Tel: (+86)13019705608

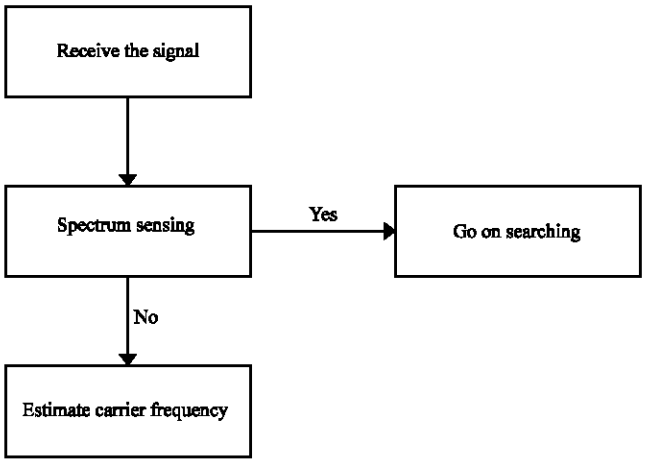

Fig. 1: Overall structure diagram of S-band uplink electronic surveillance

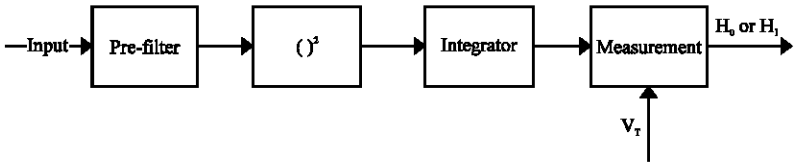

Fig. 2: Classical time-domain energy detection

The signal modulated by BPSK can be written as car = carr.cos ($2\pi f_c t$), where carr is the baseband code sequence, f_c is subcarrier; the whole signal is:

$$x(t) = \cos(2\pi f_{sc} t + m_p car)$$

where, f_{sc} is carrier, m_p is phase modulation ratio.

The classical algorithm: The situation of interest is shown in Fig. 2. The energy detector consists of a square law device followed by finite time integrator. The output of the integrator at any time is the energy of the input to the squaring device over the interval T in the past (Hao and Zu, 2009). The pre-filter serves to limit the noise bandwidth; the noise at the input to the squaring device has a band-limited, flat spectral density.

The detection is a test of the following two hypotheses. (a) H_0: The input y(t) is noise alone: y(t) = n(t); (b) H_1: The input y(t) is signal plus noise: y(t) = n(t)+s(t). The output of the integrator is denoted by V which will be compared with V_T. If $V>V_T$, it represents that there exists primary users (that is H_1); or $V<V_T$, it represents that there doesn't exist any primary users (that is H_0).

According to the sampling theorem, the noise and signal process can be expressed as (Dotlic and Kohno, 2011):

$$n(t) = \sum_{i=1}^{2TW} a_i \text{sinc}(2Wt - i), 0 < t < T, a_i = n(\frac{i}{2W}) \quad (1)$$

$$s(t) = \sum_{i=1}^{2TW} a_i \text{sinc}(2Wt - i), 0 < t < T, a_i = s(\frac{i}{2W}) \quad (2)$$

$$b_i = \frac{a_i}{\sqrt{2WN_{02}}} \quad (3)$$

$$\beta_i = \frac{a_i}{\sqrt{2WN_{02}}} \quad (4)$$

- When there is no signal, that is H_0, y(t) = n(t):

$$V = \int_0^T y^2(t)dt / N_{02} = \sum_{i=1}^{2TW} a_i^2 / (2WN_{02}) = \sum_{i=1}^{2TW} b_i^2 \quad (5)$$

So V can be viewed as the sum of the squares of 2TW standard Gaussian variables with zero mean and unit variance. Therefore, V follows a central Chi-square distribution with 2TW degrees of freedom.

- When there exists signal, that is H_1, y(t)=n(t)+s(t):

$$y(t) = \sum_{i=1}^{2TW} (a_i + a_i) \text{sinc}(2Wt - i) \quad (6)$$

$$\int_0^T y^2(t)dt = \sum_{i=1}^{2TW} (a_i + a_i)^2 \quad (7)$$

Then:

$$V = \int_0^T y^2(t)dt / N_{02} = \sum_{i=1}^{2TW} (b_i + b_i)^2 \quad (8)$$

Where:

$$l = \sum_{i=}^{2TW} b_i^2 = \int_o^T s^2(t)dt / N_{02} = E_s / N_{02} \quad (9)$$

So the decision statistic V in this case will have a non-central χ^2 distribution with 2TW degrees of freedom and a non centrality parameter λ. Following the short-hand notations mentioned in the beginning of this section, we can describe the decision statistic as:

$$V \sim \begin{cases} \chi^2_{2TW} & , H_0 \\ \chi^2_{2TW}(\lambda) & , H_1 \end{cases}$$

The detection probability Q_d and false probability Q_f can be written as follows:

$$Q_d = \text{Prob}\{V > V_T \mid H_1\} = \text{Prob}\{c^2_{2TW}(l) > V_T\} \quad (10)$$

$$Q_f = \text{Prob}\{V > V_T \mid H_0\} = \text{Prob}\{c^2_{2TW} > V_T\} \quad (11)$$

where, s(t) is signal waveform, n(t) is noise waveform, T is observation time interval, W is bandwidth, λ is the ratio of signal to noise, N_0^2 is two-side noise power density spectrum and V_T is the threshold.

The modified algorithm: Most of the articles about energy detection concentrate on the process of noise and dual-threshold (Kalamkar and Banerjee, 2013; Song *et al*., 2010; Wu *et al*., 2009) while few pay attention to the main algorithm. Due to the disadvantage of the classical energy detection algorithm, in this study the squaring device and the threshold setting in frequency domain are modified as follows. Figure 3 shows classical frequency-domain energy detection algorithm and Fig. 4 shows modified frequency-domain energy detection algorithm which is proposed in this study.

As is known that the amplitude of the received signal represents the size of the margin of the received signal, the sum of the square represents the energy of the received signal and the coefficient of kurtosis (the fourth order) reflects the concentration and dispersion of random variables (the degree of tip level). Here coefficient of kurtosis is adopted to describe the degree of centralization and decentralization of signal. As a result, it is easy to find out the maximum of the signal spectrum in frequency domain (Zhao and Swami, 2007; Zhao *et al*., 2010). When noise is only input:

$$\begin{aligned} N(w) &= \sum_i^{2TW} a_i \hat{\phi}(\frac{w}{2W})(\frac{1}{2W}) \exp(-jiw) \\ &= \hat{\phi}(\frac{w}{2W})(\frac{1}{2W}) \sum_i^{2TW} a_i \exp(-jiw) \end{aligned} \quad (12)$$

where, $\phi(x) = \text{sinc}(x)$, $\hat{\phi}(w)$ is the Fourier transform of $\phi(x)$ and $j^2 = -1$. Then the amplitude of noise can be described as:

$$|N(w)|^2 = |\hat{\phi}(\frac{w}{2W})|^2 (\frac{1}{2W}) \sum_i^{2TW} |a_i|^2 \quad (13)$$

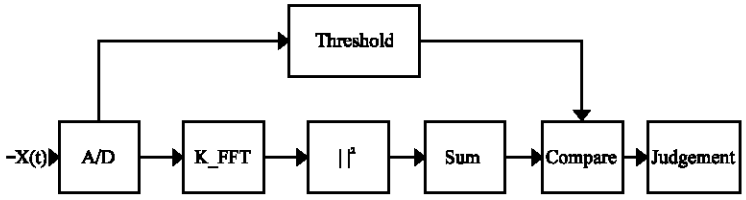

Fig. 3: Classical frequency-domain energy detection

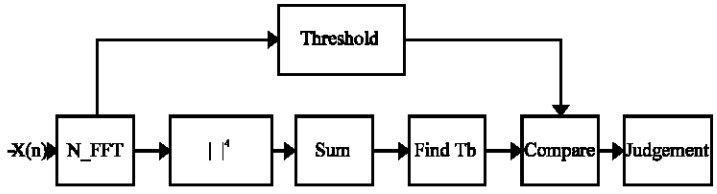

Fig. 4: Modified frequency-domain energy detection

The same approach is applied when the signal s(t) is present, then:

$$S(w) = \hat{\phi}(\frac{w}{2W})(\frac{1}{2W})\sum_{i}^{2TW}\alpha_i \exp(-jiw) \tag{14}$$

$$|S(w)|^2 = |\hat{\phi}(\frac{w}{2W})|^2 (\frac{1}{2W})\sum_{i}^{2TW}|\alpha_i|^2 \tag{15}$$

$$\lambda = \frac{\sum|S(w)|^2}{\sum|N(w)|^2} = \frac{|S_{eq}(w)|^2 B_c}{|N_{eq}(w)|^2 B_{ss}} = \frac{|S_{eq}(w)|^2 \varepsilon B_{ss}}{|N_{eq}(w)|^2 B_{ss}} = \frac{|S_{eq}(w)|^2 \varepsilon}{|N_{eq}(w)|^2}$$
$$\Rightarrow \frac{|S_{eq}(w)|^2}{|N_{eq}(w)|^2} = \frac{\lambda}{\varepsilon} \tag{16}$$

where, λ is signal to noise ratio, $S_{eq}(w)$ and $N_{eq}(w)$ is separately the equivalent value of S(w) and N(w), B_c and B_{ss} is the bandwidth of signal and noise separately and $B_{ss} = \varepsilon B_s$, that is to say $0 \le \varepsilon \le 1$.

We denote Th_1 and Th_2 as:

$$Th\_1 = \frac{|S(w)|^2}{|N(w)|^2} = \frac{\lambda}{\varepsilon} \text{ and } Th\_2 = \frac{|S(w)|^4}{|N(w)|^4} = \left(\frac{\lambda}{\varepsilon}\right)^2$$

When Th_1>1, that is to say $\lambda \ge \varepsilon$, Th_2>Th_1. It means that the kurtosis algorithm can make the signal notable among the noise and it's also confirmed by the following simulation results. In fact, the signal is a kind of narrowband signal. If we set $\frac{\lambda}{\varepsilon}$ as the classical signal to noise ratio, $\left(\frac{\lambda}{\varepsilon}\right)^2$ is the modified signal to ratio, then the improvement in SNR(dB) is:

$$\Delta SNR = 10\log\left(\frac{\lambda}{\varepsilon}\right)^2 - 10\log\left(\frac{\lambda}{\varepsilon}\right) = 10\log(\lambda) - 10\log(\varepsilon) \tag{17}$$

Figure 5 shows the spectrum of ideal signal, where there is no noise. Figure 6 shows the spectrum of signal which noise is added into. From Fig. 5 and 6, we can see that the useful signal is drawn in the noise. Figure 7 shows the modified signal spectrum, where the fourth order of signal is used. Compared with Fig. 6, we can see that the useful signal is more obvious from the background noise in Fig. 7. The result is the same as Eq. 17: using the fourth order instead of square can make the useful signal more obvious from the background noise.

In classical energy detection algorithm, the threshold is a single-value or dual, so when background noise changes, the threshold has to be changed. However a ratio threshold is developed in this paper which can void the influence of the noise changes:

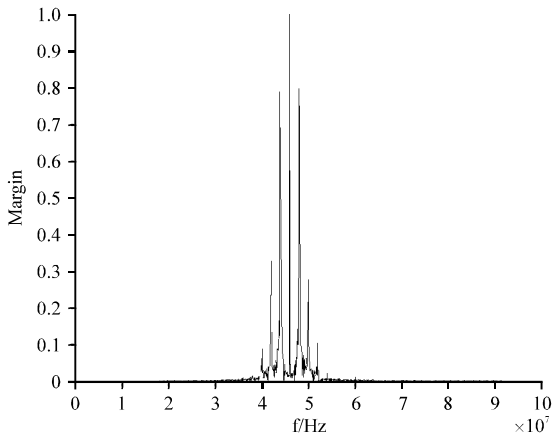

Fig. 5: Ideal signal spectrum

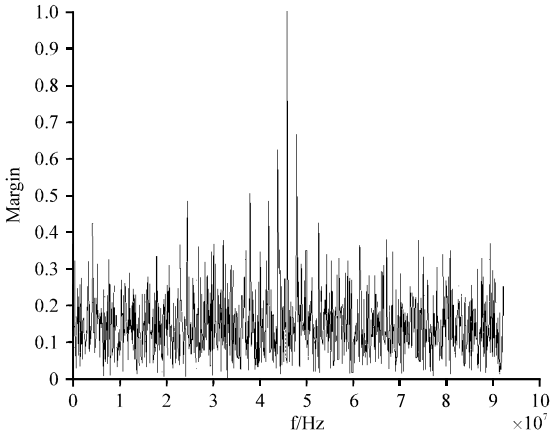

Fig. 6: Actual signal spectrum

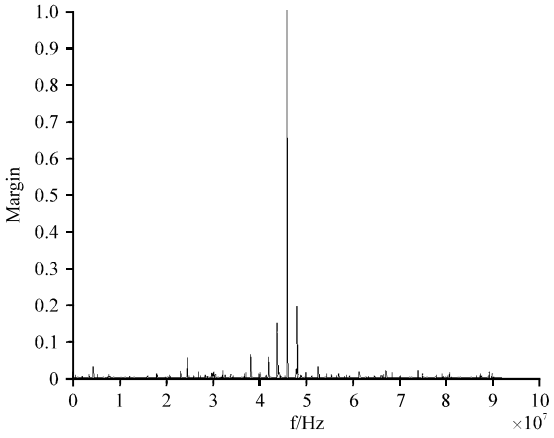

Fig. 7: Modified signal spectrum

- First, input noise only and FFT it, then calculate the fourth order

- Secondly, the spectrum is divided into fixed bandwidth groups and sum each group, denoted by S_k
- Thirdly, find the maximum value among S_k and denoted by S_m, then the rest of S_k denoted by S_e
- Fourthly, take the average of S_m and Se separately and then defined R as both the ratio of S_m and S_e
- Fifthly, carry out the Monte Carlo simulation 10,000 times
- Finally, after sorting the results, we can obtain correspondence between the threshold and the probability of false alarm

From Fig. 8, when there is noise only, R is very low; while when there exist signal and noise together, R will become obviously higher than before which means that mean of signal only and mean of signal with noise can be easily separated from each other. It is obvious that when the SNR is too low, the modified algorithm does not work, too. It can be explained in "SNR Wall" theories. Somebody may say why you don't use the eighth order. In fact, if we use the fourth order to simulate, we need to simulate about 3N more multiplication than classical algorithm; if we use the eighth order, we have to simulate about 7N more multiplication than algorithm (N is the number of FFT). The larger N is, the more complex the eighth order is and the more time it will cost, at the same time it can't improve the algorithm forever because of the "SNR Wall" theory (Mariani *et al*., 2011; Ji and Zhu, 2010). Taking these factors into account, kurtosis is used to modify the algorithm.

In fact, R in Fig. 8 is just the ratio threshold in our algorithm. The ratio threshold should be between 2 and 10 and the simulation result is showed below. In Table 1, SNR is the ratio of signal and noise and R denotes the threshold. When the threshold R is too low, for example R = 3, the false alarm probability P_f is higher than 90%. And P_f becomes lower as R becomes higher. It's obvious to see that when ratio threshold is 9 or 10, the false alarm probability can be lower than 5%. If the threshold is higher, the missed alarm probability will be higher, too, so we choose threshold = 9 or 10.

"Adding windows" way to estimate the carrier frequency: Besides all the things mentioned above, this paper also proposes an "adding windows" way to estimate the central frequency.

Butterworth filter has monotonic and smooth frequency characteristics, but under the same transition bandwidth conditions, the higher the required filter order results in the higher corresponding costs; Chebyshev filter has ripples in pass-band or resistance, but under the same pass-band conditions, the required filter order is lower. Although the type I Chebyshev analog prototype filter has a narrower, steeper transition zone, this feature is at the expense of the smooth monotonic pass-band characteristics (and results in ripples). So we choose type II Chebyshev filter.

For type I Chebyshev filters and type II Chebyshev filters, the gain (or amplitude) response as a function of angular frequency ω of the nth-order low-pass filter is given by:

$$G_n(w) = |H_n(jw)| = \frac{1}{\sqrt{1+\varepsilon^2 T_n^2(\frac{w}{w_0})}} \quad (18)$$

$$G_n(w, w_0) = \frac{1}{\sqrt{1+\frac{1}{\varepsilon^2 T_n^2(\frac{w_0}{w})}}} \quad (19)$$

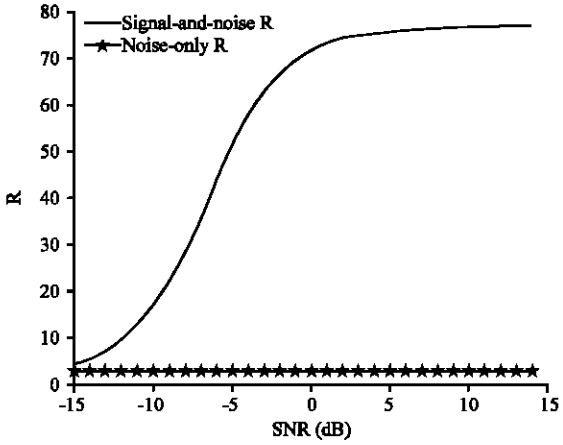

Fig. 8: Correlation between threshold R and SNR

Table 1: Under different thresholds R, correlation between false alarm probability and SNR

SNR (R)	-20 dB	-18 dB	-16 dB	-14 dB	-12 dB	-10 dB	-8 dB	-6 dB	-4 dB	-2 dB	0 dB
2	1	1	1	1	1	1	1	1	1	1	1
3	0.97	0.973	0.961	0.971	0.969	0.971	0.961	0.964	0.962	0.971	0.97
4	0.711	0.703	0.684	0.702	0.693	0.693	0.716	0.693	0.697	0.720	0.68
5	0.42	0.429	0.413	0.416	0.418	0.424	0.414	0.408	0.419	0.413	0.39
6	0.209	0.213	0.218	0.224	0.232	0.212	0.242	0.202	0.229	0.194	0.20
7	0.105	0.124	0.102	0.095	0.111	0.116	0.114	0.121	0.125	0.118	0.10
8	0.064	0.043	0.076	0.068	0.053	0.068	0.078	0.071	0.061	0.075	0.07
9	0.027	0.026	0.035	0.038	0.037	0.033	0.032	0.04	0.031	0.038	0.03
10	0.018	0.016	0.015	0.019	0.018	0.027	0.021	0.025	0.027	0.010	0.02

where, ε is the ripple factor, ω_0 is the cutoff frequency and $T_n(x)$ is Chebyshev polynomial of the nth order with variable x.

Make the input signal pass through a few groups of "window" filters and each group has a different center frequency. Find out which group's output energy is the maximum, then divide this group's bandwidth again into new groups and go on as the first step. At last, we use the last filter's center frequency to estimate the input signal's center frequency.

SIMULATION AND ANALYSIS

Input PCM-PSK-PM signal: Generally speaking, paper will set the signal modulated by BSK, FM or any other. After all, they just pay attention to the algorithm itself and have no background of application. In this paper, we use the system to simulate S-band uplink electronic surveillance. Depending on the particular background of application in this study, the signal of this paper is multi-modulated by PCM-PSK-PM and the variables are set as follows: the baseband code rate is 200 kHz, the subcarrier is 2 MHZ, the main carrier is 2070MHz, m_p is 1.5 and sampling frequency is 184MHz.

Figure 9 shows the PCM-PSK-PM signal in frequency domain which is used for simulation later. After undersampling by 184 MHZ, carrier frequency of signal can be moved to 46 MHZ which can be got as Eq. 20:

$$2070\text{-}184\times11 = 46\ \text{MHZ} \quad (20)$$

Detection performance of the modified algorithm: Above in Table 2 and 3, respectively, when threshold = 9 and threshold = 10, the false alarm probability P_f and undetected probability P_m and the error probability P_e (the sum of P_f and P_m) are measured. According to Table 2 and 3, we can find that, when threshold = 9, the error probability P_e can be about 5% at -10dB, while the P_e is only 0.074 when threshold = 10. However if SNR become higher than -8dB, the performance under threshold = 10 is better than the performance under threshold = 9. It's easy to understand that the higher threshold is, the lower the P_e is. In this study, we want to make the system work well as low SNR as possible, at the same time P_e is lower than 5%. So we here take threshold = 9.

Figure 10 shows that the detection probability P_d changes with the SNR in the classical and modified energy detection algorithm. It's obvious that when SNR = 4 dB, the classical detection probability can reach 95%; however the modified algorithm shows that when even SNR = -10 dB, the detection probability can reach

Table 2: When threshold=9, detection performance of the modified algorithm

SNR (dB)	P_f (%)	P_m (%)	P_e
-20	2.5	97.5	1
-18	2.8	97.2	1
-16	3.5	97.5	1
-14	3.8	88.5	0.923
-12	3.7	43.2	0.469
-10	3.3	2.2	0.055
-8	3.2	0.0	0.032
-6	4.0	0.0	0.040
-4	3.1	0.0	0.031
-2	3.8	0.0	0.038
0	2.7	0.0	0.027

Table 3: When threshold=10, detection performance of the modified algorithm

SNR(dB)	P_f (%)	P_m (%)	P_e
-20	1.8	98.2	1
-18	1.6	98.4	1
-16	1.5	98.5	1
-14	1.9	92.1	0.940
-12	1.8	50.5	0.523
-10	2.7	4.7	0.074
-8	2.1	0.0	0.021
-6	2.5	0.0	0.025
-4	2.7	0.0	0.027
-2	1.0	0.0	0.010
0	2.2	0.0	0.022

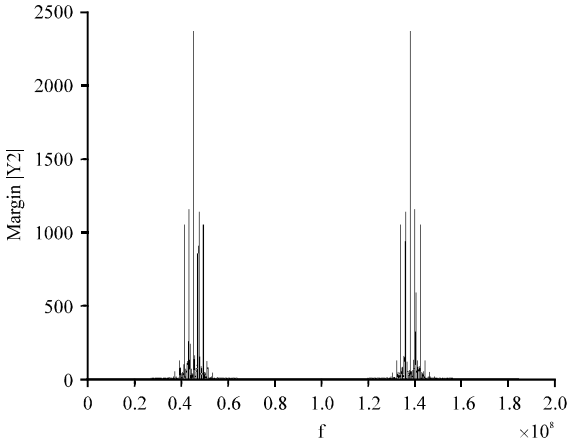

Fig. 9: PCM-PSK-PM signal in frequency domain

95% and meanwhile the error probability is less than 5%. So the improved algorithm is at least 10 dB better than the classical energy detection algorithm. In theory, according to Eq. 14, ε is about 0.25, so the improvement is about $10\log(\varepsilon) = 14$ dB. The two results coincide. In this study Song *et al.* (2010) which uses two thresholds for energy detection, the detection probability can reach about 95% at SNR = -7dB which is not better than the result of this study. The algorithm just needs one threshold. Since the variability only needs to compare with threshold just once, it will be faster than two thresholds algorithm and it will not leave signal into area of uncertainty as two

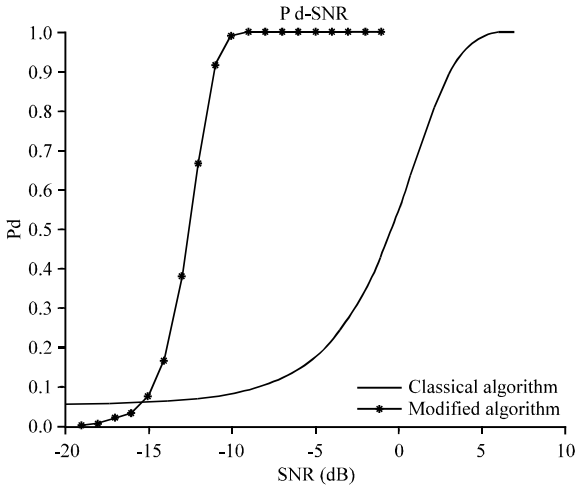

Fig. 10: P_d-SNR in classical and modified algorithm separately

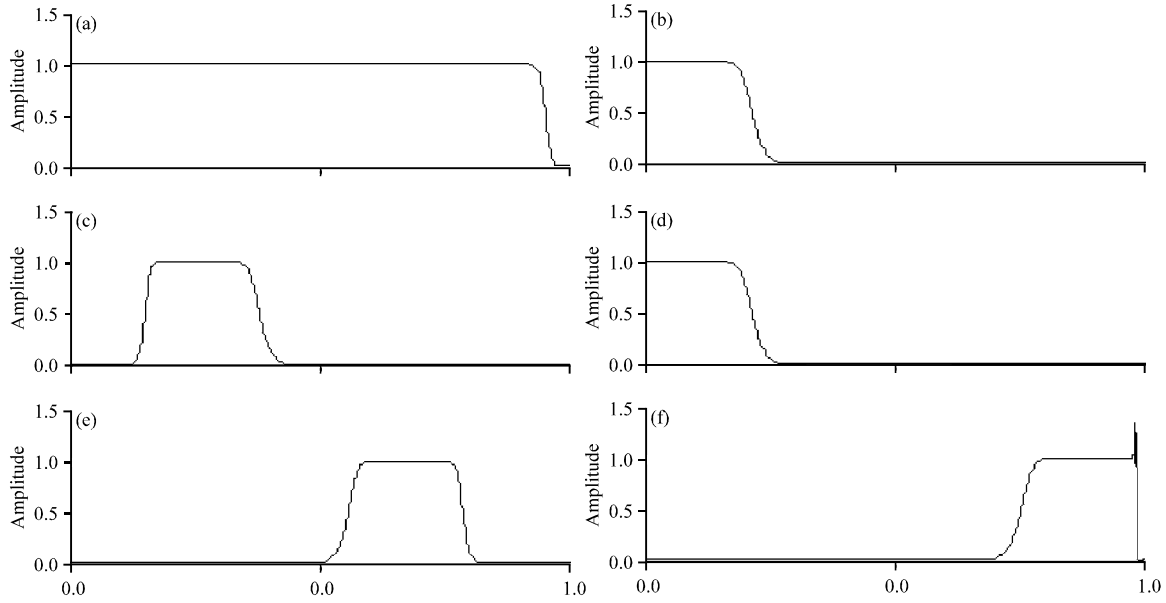

Fig. 11(a-f): Filters in digital domain, (a) All-pass filter, (b) The first component of filter (a), (c) The second component of filter (a), (d) The third component of filter (a), (e) The fourth component of filter (a) and (f) The fifth component of filter (a)

thresholds algorithm. Meanwhile, most previously published studies just pay attention to false alarm probability P_f without considering undetected probability P_m. In fact, we should take total error probability P_e in account which is the sum of P_f and P_m which is used in this study.

Estimate the center frequency of the carrier signal: We use an "adding windows" way to confirm carrier frequency which consists of a set of filters. Figure 11 shows the frequency range of six filters in digital domain. In Fig. 11a shows an all-pass filter in digital domain (b)~(f) show filters of different frequency in digital domain. It can be considered that filter (a) is separated into filters (b)~(f). In simulation of this study, we find that signal that passes through filter (d) has the maximum of energy. It is clear that the carrier frequency is in the range of this filter. Then filter (d) is separated into new filters just as what is done to filter (a) above. At last, we can get the carrier frequency by the last filter's center frequency. In Fig. 12a shows the

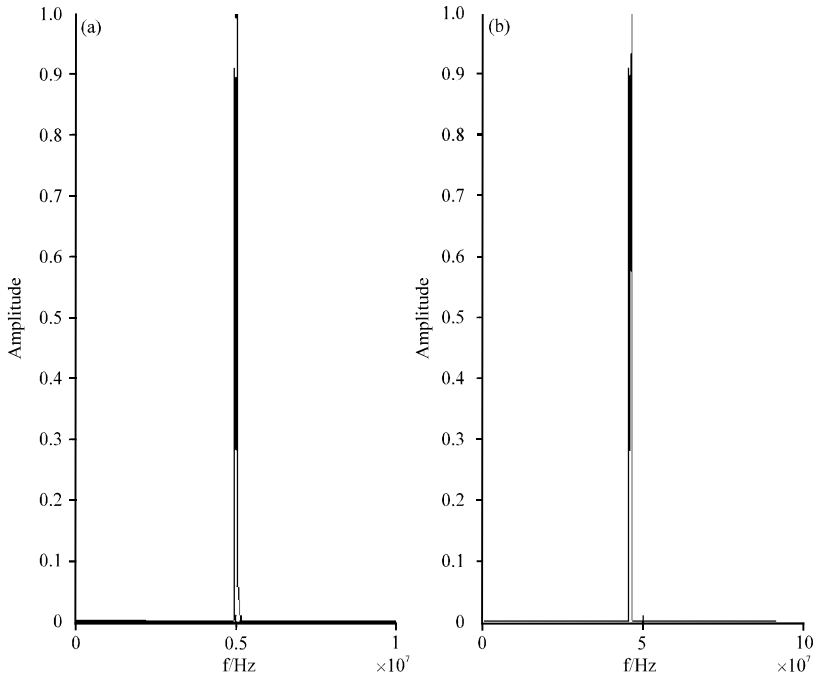

Fig. 12(a-b): Estimation of carrier frequency, (a) Carrier frequency in digital domain and (b) Carrier frequency in frequency domain

last filter's center frequency in digital domain and (b) shows the same result in frequency domain. From (b) of Fig. 12, we can see that the estimate of carrier frequency is 2070. 0275 MHZ which is obtained by the inverse of Eq. 14 and the error of estimation is only 0.0275 MHZ.

CONCLUSION

The main contribution of this study is that energy detection algorithm in cognitive radio spectrum sensing technology has been improved and an "adding windows" way is proposed to confirm the signal's center frequency. After simulation on the S-band monitoring and control signal, we come up with the conclusion that the improved energy detection method can effectively overcome the shortcomings of the classical energy detection method which is sensitive to background noise. The measuring results show that the improved algorithm is at least 10 dB better than the classical energy detection algorithm and the error of carrier frequency estimation is only 0.0275 MHZ.

REFERENCES

Appadwedula, S., V.V. Veeravalli and D.L. Jones, 2008. Decentralized detection with censoring sensors. IEEE Trans. Signal Process., 56: 1362-1373.

Chen, Q., M. Motani, W.C. Wong and A. Nallanathan, 2011. Cooperative spectrum sensing strategies for cognitive radio mesh networks. IEEE J. Selected Topics Signal Process., 5: 56-67.

Dotlic, I. and R. Kohno, 2011. Application of IEEE 802.15. 6 IR UWB physical layer for medical BAN. Int. J. Ultra Wideband Commun. Syst., 2: 104-115.

Hao, J.W. and Y.X. Zu, 2009. An enhanced energy detection algorithm in cognitive radio. Proceedings of the 5th International Conference on Wireless Communications, Networking and Mobile Computing, September 24-26, 2009, Beijing, pp: 1-4.

Ji, G. and H. Zhu, 2010. On the noise power uncertainty of the low SNR energy detection in cognitive radio. J. Comput. Inf. Syst., 6: 2457-2463.

Kalamkar, S.S. and A. Banerjee, 2013. Improved double threshold energy detection for cooperative spectrum sensing in cognitive radio. Defence Sci. J., 63: 34-40.

Liang, G., R. Agarwal and N. Vaidya, 2010. When watchdog meets coding. Proceedings of the IEEE INFOCOM, March 14-19, 2010, San Diego, CA., USA., pp: 1-9.

Maleki, S. and G. Leus, 2013. Censored truncated sequential spectrum sensing for cognitive radio networks. IEEE J. Selected Areas Commun., 31: 364-378.

Mao, S. and T. Wolf, 2010. Hardware support for secure processing in embedded systems. IEEE Trans. Comput., 59: 847-854.

Mariani, A., A. Giorgetti and M. Chiani, 2011. SNR wall for energy detection with noise power estimation. Proceedings of the IEEE International Conference on Communications, June 5-9, 2011, Kyoto, Japan, pp: 1-6.

Mitola III, J., H.H. Zheng and K.R. Chowdhury, 2012. Editorial for special issue on cognitive radio ad hoc networks. Ad Hoc Networks, 10: 737-739.

Ozdemir, O., Z. Sahinoglu and J. Zhang, 2008. Narrowband interference resilient receiver design for unknown UWB signal detection. Proceedings of the IEEE International Conference on Communications, May 19-23, 2008, Beijing, China, pp: 785-789.

Song, C., Y.D. Alemseged, H.N. Tran, G. Villardi, C. Sun, S. and H. Harada, 2010. Adaptive two thresholds based energy detection for cooperative spectrum sensing. Proceedings of the 7th IEEE Consumer Communications and Networking Conference, January 9-12, 2010, Las Vegas, NV., USA., pp: 1-6.

Wang, P., J. Fang, N. Han and H. Li, 2011. Rapid spectrum sensing with multiple antennas for cognitive radio. Proceedings of the IEEE AFRICON, September 13-15, 2011, Livingstone, Zambia, pp: 1-6.

Wu, J.B., T. Luo, J.F. Li and G.X. Yue, 2009. A cooperative double-threshold energy detection algorithm in cognitive radio systems. Proceedings of the 5th International Conference on Wireless Communications, Networking and Mobile Computing, September 24-26, 2009, Beijing, pp: 1-4.

Zhao, Q. and A. Swami, 2007. A survey of dynamic spectrum access: signal processing and networking perspectives. Proceedings of the IEEE International Conference on Acoustics, Speech and Signal Processing, Volume 4, April 15-20, 2007, Honolulu, HI., USA., pp: IV-1349-IV-1352.

Zhao, Y., S. Li, N. Zhao and Z. Wu, 2010. A novel energy detection algorithm for spectrum sensing in cognitive radio. Inform. Technol. J., 9: 1659-1664.